J. Cent. South Univ. (2022) 29: 836−847
DOI: https://doi.org/10.1007/s11771-022-4969-x

Springer

Effects of pre-rolling on mechanical properties and fatigue crack growth rate of 2195 Al-Li alloy

CHEN Meng-xi(陈梦喜)[1], LI Yi-bo(李毅波)[2]*, XIA Lin-yan(夏琳燕)[1], HUANG Ming-hui(黄明辉)[2], WU Zhen-yu(吴镇宇)[3], YANG Yi(杨义)[1], QU Zi-jing(屈子敬)[1]

1. School of Mechanical and Electrical Engineering, Central South University, Changsha 410083, China;
2. Light Alloy Research Institute, Central South University, Changsha 410083, China;
3. Guangxi Liuzhou Yinhai Aluminum Company Limited, Liuzhou 545006, China

Abstract: While pre-deformation is often conducted before aging treatment to increase the strength and microhardness of 2195 Al-Li alloy, it often increases the fatigue crack growth (FCG) rate and thus reduces the fatigue life of the alloy. To determine the effects and causes of pre-deformation and heat treatment on the mechanical properties and FCG rate of 2195 Al-Li alloy, and to provide a suitable calculation model for the FCG rate under different pre-deformation conditions, 2195 Al-Li alloy specimens with different degrees of pre-rolling (0, 3%, 6%, and 9%) were investigated. The experimental results indicate that with the increase of pre-rolling, the density of the T_1 phase and the uniformity of the S' distribution and the microhardness, tensile strength, and yield strength of the alloy increase and at the same time the FCG rate increases, and thus the fatigue life is reduced. It was also found that the normalized stress intensity factor of elastic modulus (E) can be applied to correlate the FCG rate of pre-rolled 2195 Al-Li alloy with constant C and K parameters.

Key words: 2195 Al-Li alloy; pre-rolling; over-aging; fatigue crack growth; mechanical properties

Cite this article as: CHEN Meng-xi, LI Yi-bo, XIA Lin-yan, HUANG Ming-hui, WU Zhen-yu, YANG Yi, QU Zi-jing. Effects of pre-rolling on mechanical properties and fatigue crack growth rate of 2195 Al-Li alloy [J]. Journal of Central South University, 2022, 29(3): 836−847. DOI: https://doi.org/10.1007/s11771-022-4969-x.

1 Introduction

Due to their low density, high strength, high specific stiffness, and excellent toughness [1 − 3], third-generation Al-Li alloys are widely used in the aerospace industry [4, 5]. For example, 2195 Al-Li alloy was used by NASA in a cryogenic propellant storage tank for the space shuttle [6], and is commonly applied to the fuselage frame and wing skin of spacecraft, etc.

Thermomechanical treatment, such as pre-deformation followed by aging or over-aging treatment, is usually used to achieve good mechanical properties, fatigue properties, and microstructures of Al-Li alloys [7].

Generally, pre-deformation can increase the dispersion of fine T_1 phases in Al-Li alloys and lead to the increase of both the tensile and yield strengths of the alloys, but it often reduces the plasticity [8−10] and fatigue resistance [11, 12]. WANG et al [13] found that the micro-crack defects and fatigue crack growth (FCG) rate of 2E12 alloy were increased by pre-stretching, and thus the fatigue life of the alloy was reduced. LIU et al [14] indicated that pre-

Foundation item: Project(U21A20132) supported by the National Natural Science Foundation of China; Project(GuiRenzi2019(13)) supported by the Guangxi Specially-invited Experts Foundation of Guangxi Zhuang Autonomous Region, China
Received date: 2021-09-13; **Accepted date:** 2022-01-31
Corresponding author: LI Yi-bo, PhD, Professor; E-mail: yibo.li@csu.edu.cn; ORCID: http://orcid.org/0000-0002-2408-9148

rolling had a greater effect on the FCG rate in stage II (the Paris zone) than the pre-stretching method. SHEN et al [15] found that the low-cycle fatigue life of 2195-T8 Al-Li alloy decreased with the increase of pre-deformation, but the high-cycle fatigue life was only slightly changed.

To date, there have been numerous studies on the effect of pre-deformation on the mechanical strength of Al-Li alloys [16 − 19], but few investigations have focused on the effects of pre-deformation on the FCG rate and fatigue resistance; thus, it is difficult to determine the degree of pre-deformation and predict the fatigue life under different pre-deformation conditions. In the present work, the effects of pre-rolling on the FCG rate (in the Paris zone) and microstructure of 2195 Al-Li alloy were experimentally studied to reveal the influence of the microstructure on the FCG rate. Furthermore, the relationship between the degree of pre-rolling and the fatigue life was established, and normalized stress intensity factors were correlated with the FCG rate, which will aid in the determination of the fatigue life of pre-rolled 2195 Al-Li alloys after the over-aging process.

2 Materials and methods

The studied 2195 Al-Li alloy was in the form of a plate, which had a thickness of 2.18 mm and was in the O-temper state. The chemical composition of the alloy is reported in Table 1.

Table 1 Chemical composition of 2195 Al-Li alloy (wt.%)

Cu	Mg	Li	Ag	Zr	Al
4.12	0.44	1.02	0.4	0.11	Balance

Considering that 2195 Al-Li alloy is often used in the T8 temper state, the original 2195-O Al-Li alloy was first treated by solid solution at 530 °C for 60 min and subsequently water quenched at room temperature (RT). After pre-rolling by 0, 3%, 6%, and 9%, respectively, artificial aging was conducted at 160 °C for 96 h. To minimize the influence of natural aging on various properties of the alloy, pre-rolling treatment was carried out within 10 min after quenching, and over-aging heat treatment was carried out within 1 h after quenching. The thermomechanical histories of the non-pre-deformed and pre-rolled specimens are presented in Figure 1.

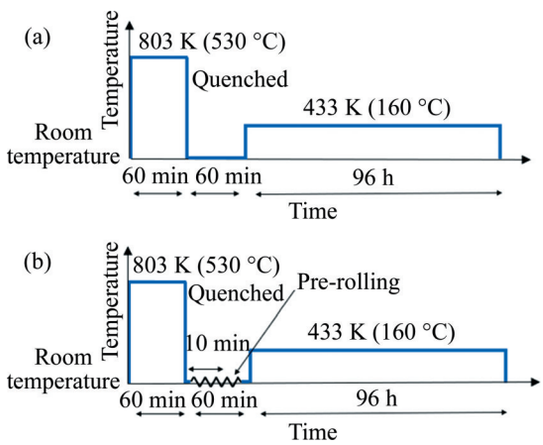

Figure 1 Thermomechanical histories of specimen without pre-rolling (a) and specimens subjected to different degrees of pre-rolling (b)

After over-aging treatment, the eight aluminum alloy plates were cut into the required shapes for hardness, tensile, and fatigue tests. The geometry of the fatigue test specimens is exhibited in Figure 2. Before testing, each specimen was sanded with waterproof abrasive paper and polished to meet the GB/T6398—2017 standard, and was then cleaned with an ultrasonic cleaning machine.

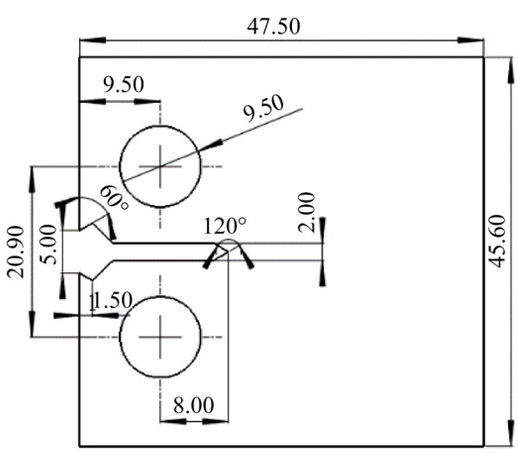

Figure 2 Geometry of fatigue test specimens (unit: mm)

Vickers hardness measurements were carried out using an HYV-1000 digital micro-Vickers hardness tester. Seven test points for each specimen were chosen for the hardness tests; after omitting the maximum and minimum values, the hardness of the specimens was determined from the average of the remaining five test points. Then, the mechanical tensile tests of the specimens with different degrees

of pre-rolling were performed at RT by an MTS-810 testing machine with a tension speed of 2 mm/min. Each test was performed on three specimens. The MTS-810 servo-hydraulic test system was also used for fatigue tests on the compact tensile (CT) specimens. A 2-mm initial crack was pre-fabricated on each CT specimen, after which the FCG test was carried out at RT with a constant K value of K_{max}=10 MPa·m$^{1/2}$, a maximum load of P=800 N, a cycle frequency of f=10 Hz, and a cyclic stress ratio of R=0.1. During the test, the crack length was measured using a properly calibrated direct-current potential drop (DCPD) system.

To investigate the effects of different degrees of pre-rolling on the internal precipitates of the Al-Li alloy plates, microstructure observation was carried out via high-resolution scanning transmission electron microscopy (STEM). The equipment model is Talos f200x, the selected mode is HAADF-STEM, and the inner and outer convergence half angles are 22 and 137 mrad, respectively. After the tensile and FCG tests, the fractures of the specimens were cut off for scanning electron microscopy (SEM) observation. The tensile fracture and the process of fatigue crack initiation, propagation, and breakup were observed by a field emission scanning electron microscope (TESCAN MIRA3 LMU) with a voltage of 20.0 kV.

3 Results and discussion

3.1 Influence of pre-rolling on hardness and tensile strength of 2195 Al-Li alloy specimens

As presented in Figure 3, the tensile strength, yield strength, and hardness of the 2195 Al-Li alloy specimens clearly increased with pre-rolling. Figure 3(a) reveals that the microhardness of the specimens without pre-rolling was HV 164.02, and after pre-rolling at 3%, 6% and 9%, the microhardness respectively increased by HV 7.36, HV 14.63 and HV 22.78. Furthermore, with the increase of the degree of pre-rolling from 0 to 9%, the tensile strength of the specimens increased from 555 to 641 MPa, and the yield strength increased from 519 to 605 MPa (Figure 3(b)); the tensile strength and yield strength were respectively increased by 15.5% and 14.2%. However, the elongation rate of the specimens also gradually decreased from 10.9% to 9.3% with the increase of the degree of pre-rolling from 0 to 9%.

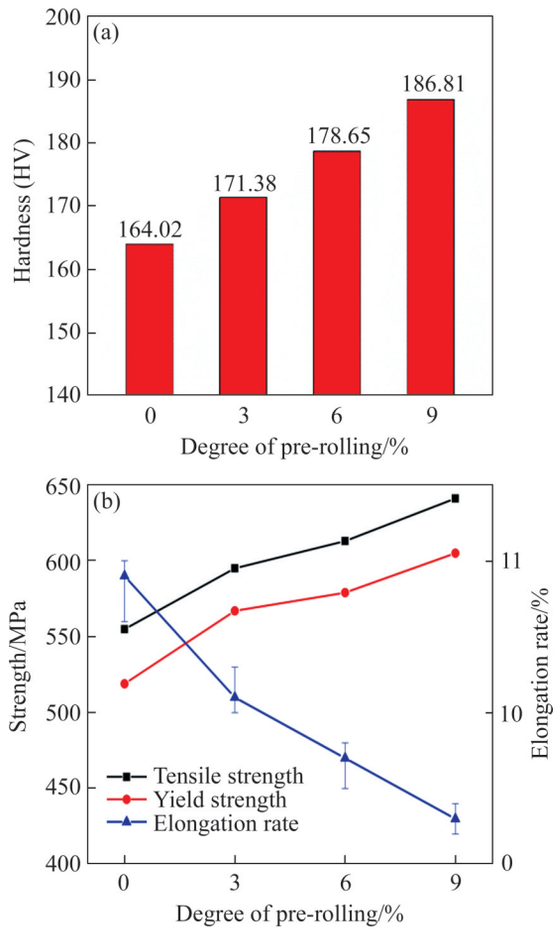

Figure 3 Mechanical properties of 2195 Al-Li alloy specimens under different degrees of pre-rolling: (a) Hardness; (b) Strength and elongation

3.2 Influence of pre-rolling on FCG rate

The experimental $a-N$ curves and the crack propagation lives of the 2195 Al-Li alloy specimens under different degrees of pre-rolling are presented in Figure 4 and Table 2. The FCG rate increased with the degree of pre-rolling, as shown in Figure 4. Compared with the non-pre-deformed specimens, the average crack propagation life of which was 67362 cycles, the average crack propagation lives of the specimens pre-rolled at 3%, 6%, and 9% were respectively 57518, 55531 and 52713 cycles, thereby reflecting respective reductions of 14.61%, 17.56% and 21.75%. In addition, Table 2 reports the 95% confidence intervals of the average value of the fatigue life of each group of alloy specimens after pre-rolling and that of the untreated specimen. Compared with the specimens without pre-rolling, the median fatigue lives of the specimens with pre-rolling degree of 3%, 6% and 9% changed by

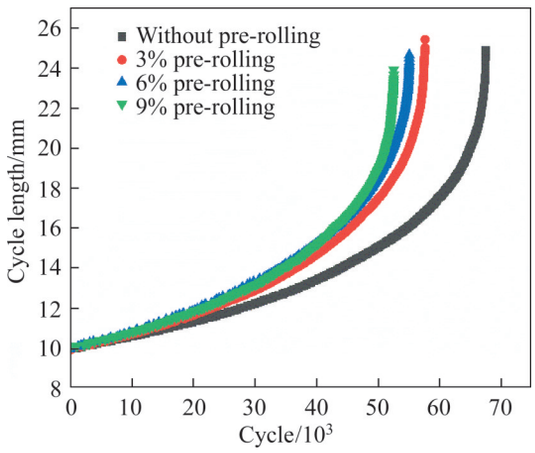

Figure 4 $a-N$ curves of 2195 Al-Li alloy specimens under different degrees of pre-rolling obtained from the fatigue tests

−23.29%– −5.94%, −29.93%– −5.2% and −35.9%– −7.59% respectively.

Figure 5 exhibits the dependence of the FCG behavior on the degree of pre-rolling, from which it is evident that pre-rolling had a significant effect on the FCG rate, especially in the far-threshold zone of crack growth. When the area between ΔK (12 − 18.5 MPa·m$^{1/2}$) was selected as the Paris area (area between the dashed purple lines in Figure 5), the average stable growth rate of the pre-rolled specimens was found to increase significantly as compared to that of the non-pre-deformed specimens.

Paris' law, namely $da/dN=C\cdot(\Delta K)^m$, can be used to calculate the FCG rate of an alloy, where a is the real-time length of the crack during crack propagation process, N is the number of cycles of alternating load during crack propagation, da/dN is the crack growth rate in the stage of stable crack propagation, K is the stress intensity factor, ΔK is the amplitude of the stress intensity factor, $\Delta K=K_{max}-K_{min}$, and C and m are material parameters.

The Paris models of the specimens under the four investigated pre-rolling conditions are given as follows.

$$\frac{da}{dN}=\begin{cases}1.079\times10^{-8}(\Delta K)^{3.767}, \\ \quad \text{non-predeformed} \\ 2.089\times10^{-8}(\Delta K)^{2.882}, \\ \quad \text{with 3\% pre-rolling} \\ 2.393\times10^{-8}(\Delta K)^{3.737}, \\ \quad \text{with 6\% pre-rolling} \\ 6.498\times10^{-8}(\Delta K)^{3.491}, \\ \quad \text{with 9\% pre-rolling}\end{cases} \tag{1}$$

Due to the variations of the values of C and da/dN with pre-deformation, it is not obvious for the values of M. The application of the traditional Paris' law to specimens with different degrees of pre-deformation is difficult. However, because the FCG and the mechanical properties, viz., the elastic

Table 2 Fatigue test results of specimens with different degrees of pre-rolling

No.	Degree of pre-rolling/%	Crack propagation life, N	Negative gain of crack propagation life ($(N-A_{average})/A_{average}$)	Median confidence interval of the fatigue life at the 95% confidence level
A_1	0	70004	—	—
A_2		64698	—	—
A_3		67383	—	—
$A_{average}$		67362	—	—
B_1	3	59943	−11.01%	(−23.29%, −5.94%)
B_2		54332	−19.34%	
B_3		58278	−13.49%	
$B_{average}$		57518	−14.61%	
C_1	6	59888	−11.10%	(−29.93%, −5.2%)
C_2		54976	−18.39%	
C_3		51728	−23.21%	
$C_{average}$		55531	−17.56%	
D_1	9	52448	−22.14%	(−35.9%, −7.59%)
D_2		48152	−28.52%	
D_3		57538	−14.58%	
$D_{average}$		52713	−21.75%	

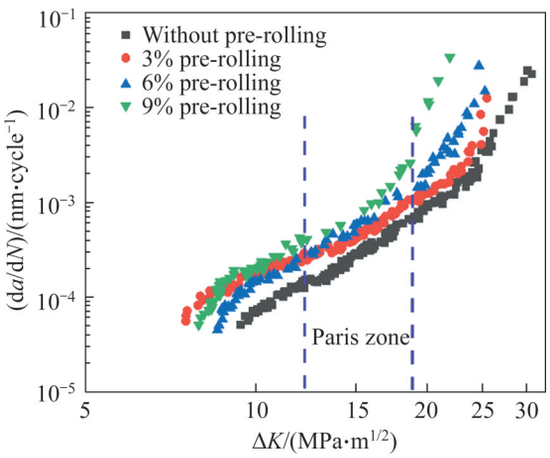

Figure 5 FCG behavior of 2195 Al-Li alloy specimens under different degrees of pre-rolling

modulus (E), yield strength (σ_y), and tensile strength (σ_b), are dependent on pre-rolling, the concept of the normalization of stress intensity factors, e.g., by replacing the value of ΔK in Paris' law with $\Delta K/E$ or $\Delta K/\sigma_b$, can be introduced to correlate the FCG data with pre-deformation. This method was initially introduced by PEARSON [20] and then successfully applied to various materials at ambient test conditions [21]. Recently, MATCHA et al [22] established a relationship between da/dN and the standardized driving force parameter $\Delta K/\sigma_y$ at different temperatures for SS316L(N) steel, as follows:

$$\frac{\mathrm{d}a}{\mathrm{d}N} = C \cdot \left(\frac{\Delta K}{\sigma_y}\right)^m \tag{2}$$

where C=4.5 nm/cycle and m=2.93 for the steel under different temperatures.

The normalized stress intensity factors $\Delta K/E$ and $\Delta K/\sigma_y$ are introduced in the present work, and the relationships between da/dN and $\Delta K/E$, and between da/dN and $\Delta K/\sigma_y$, using the data in Table 3 are respectively presented in Figure 6 and Figure 7 presents a much narrower scattering band than Figure 6; therefore, the normalized stress intensity factor $\Delta K/E$ was chosen and the Paris-type relationship between da/dN and $\Delta K/E$ was fitted as da/dN=C · $(\Delta K/E)^m$, with C=0.13 nm/cycle and m=3.59. Interestingly, the exponent is close to 3, which is the value expected based on theoretical considerations for metals and alloys [23, 24]. When E was used as the normalized stress intensity factor,

Table 3 E and σ_y values of 2195 Al-Li alloy specimens under different degrees of deformation

Deformation/%	E/GPa	σ_y/MPa
0	75.8	519
3	72.0	567
6	71.8	579
9	69.0	602

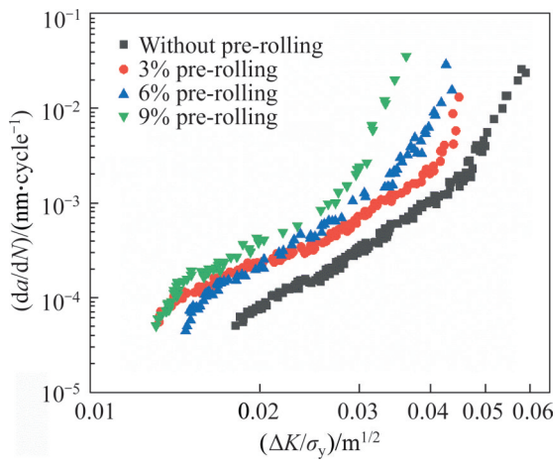

Figure 6 FCG data normalized with the yield strength of specimens under different degrees of pre-rolling

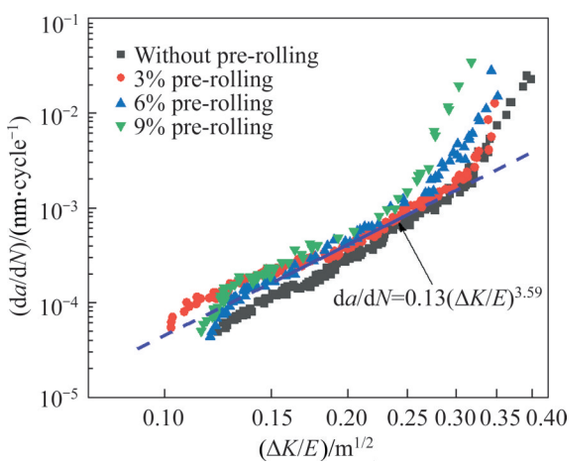

Figure 7 FCG data normalized with elastic modulus of specimens under different degrees of pre-rolling

the maximum difference of the da/dN curves of the four specimens in the Paris region was 6.3×10^{-4} mm/cycle, which is 57.74% of the maximum difference of the da/dN curves of the four specimens in the Paris region when σ_y was used as the normalized stress intensity factor.

3.3 Fracture morphology

The tensile fracture surfaces of the 2195 Al-Li alloy specimens under different degrees of pre-

rolling were observed via SEM, and the fracture morphologies are displayed in Figure 8. Based on the SEM images, all the fractures exhibited obvious layered characteristics, and the fracture type was mainly intergranular fracture. As shown in Figure 8(a), the specimen without pre-rolling had some large and deep dimples; this primarily indicates brittle fracture characteristics with some ductile fracture characteristics. With the increase of deformation to 3% (Figure 8(b), the number of dimples decreased, the depth of the dimples became shallow, and the toughness further decreased. As shown in Figure 8(c), the fracture of the specimen with 6% pre-rolling was characterized by delamination, and the dimple characteristics were no longer obvious. With the increase of deformation to 9% (Figure 8(d)), the delamination was full of fractures and the dimples disappeared. In addition, the fracture was completely occupied by a smooth interface and tearing edges.

Figure 9 presents the SEM images of the fracture morphologies in the zone of near-threshold fatigue of the 2195 Al-Li alloy specimens under the four pre-rolling conditions and reveals that the main

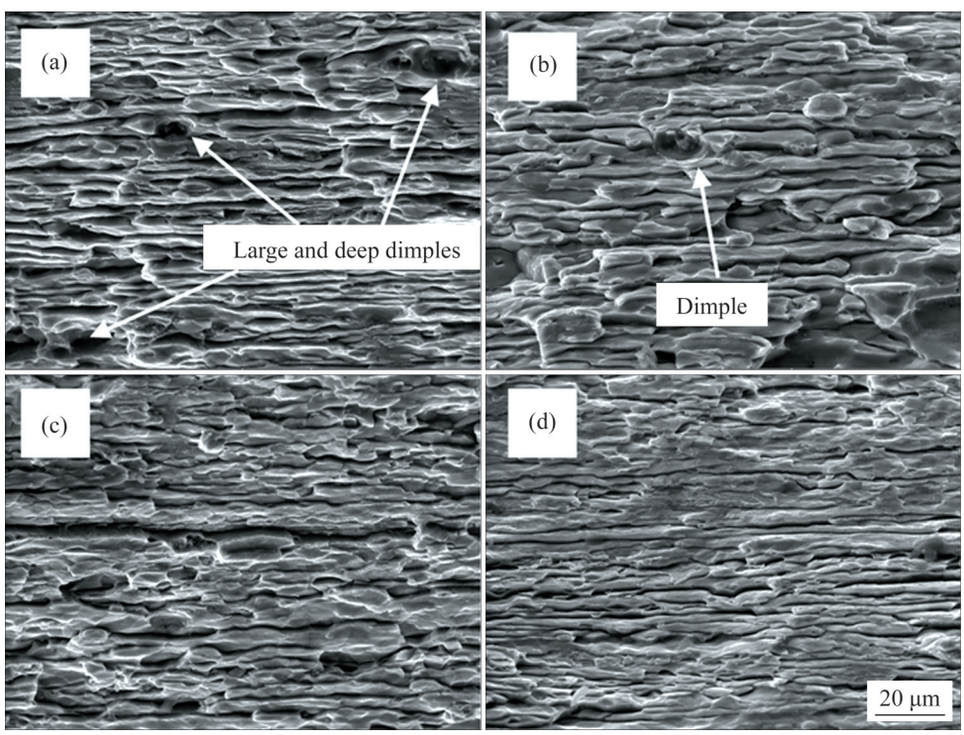

Figure 8 SEM images of fracture morphologies of 2195 Al-Li alloy specimens under different degrees of pre-rolling: (a) 0; (b) 3%; (c) 6%; (d) 9%

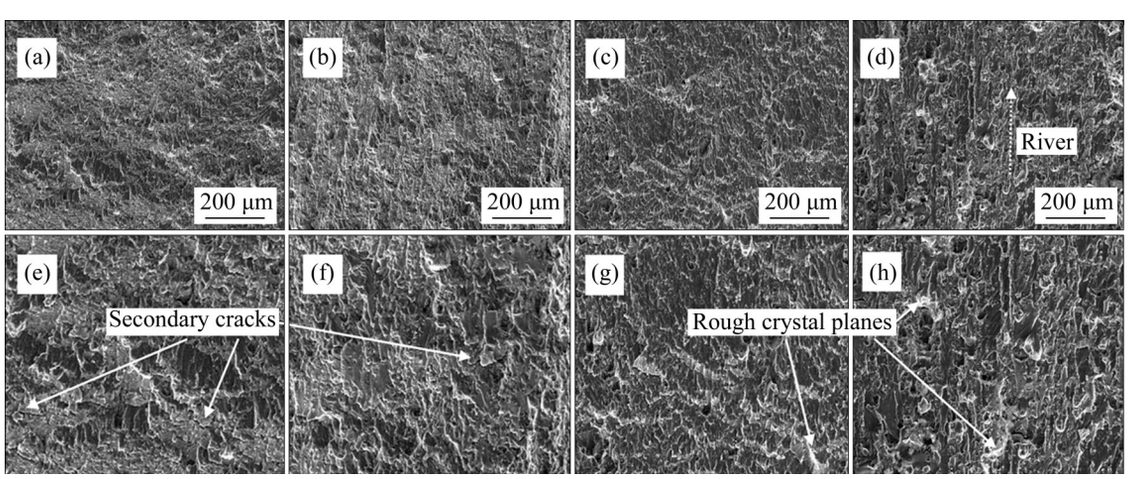

Figure 9 SEM images of fracture morphologies at near-threshold fatigue zone of 2195 Al-Li alloy specimens under different degrees of pre-rolling: (a, e) 0; (b, f) 3%; (c, g) 6%; (d, h) 9%

direction of crack propagation was from bottom to top. Rivers along the main crack propagation direction (from bottom to top) in the zone of near-threshold fatigue (Figures 9(a) – (d)) and some secondary cracks and rough crystal planes connected by tearing ridges (Figures 9(e) and (f)) of different heights were observed for the alloys under all treatment conditions.

Figure 10 displays the SEM images of the fracture surface morphologies in the Paris zone of the 2195 Al-Li alloy specimens under the four pre-rolling conditions. No obvious differences in the fatigue fracture morphologies were found under such conditions, and all specimens were characterized by intergranular fracture (Figures 10(a) – (d)) and composed of fatigue stripes and crystalline planes (Figures 11(a) – (d)). The rough surface cracks on the fracture surface

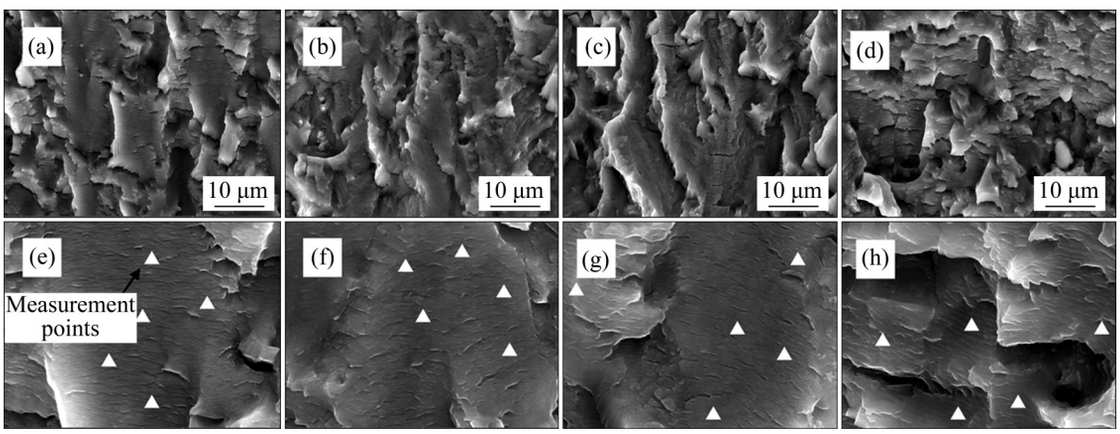

Figure 10 SEM images of fracture morphologies in Paris zone of 2195 Al-Li alloy specimens under different degrees of pre-rolling: (a, e) 0; (b, f) 3%; (c, g) 6%; (d, h) 9%

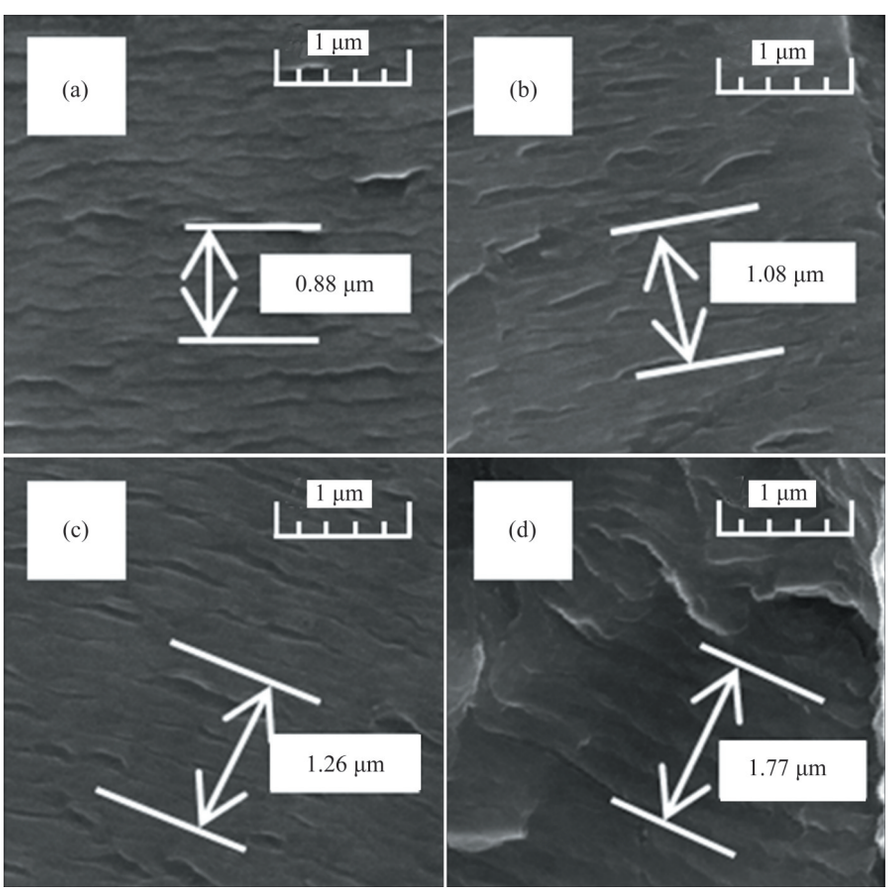

Figure 11 Morphology of fatigue stripes in Paris zone of specimens under different degrees of pre-rolling: (a) 0; (b) 3%; (c) 6%; (d) 9%

were found to propagate along different grain boundaries. In addition, it can be seen from Figures 11(a) − (d) that the fatigue stripes were slightly bent, basically parallel to each other, and roughly perpendicular to the main crack propagation direction (from bottom to top); however, the distance between two stripes varied with different degrees of pre-rolling. As present in Figures 10(e) and (h), five clear and continuous fatigue strips were selected as the measurement points of fatigue strip width. The average results of the five measurements are displayed in Figure 11 as enlarged images. The measured stripe distances for the non-pre-deformed specimen and the specimens pre-rolled at 3%, 6%, and 9% were respectively 0.88, 1.08, 1.26 and 1.77 μm. To some extent, the different stripe distances provide explanations for the different FCG rates. In the preceding measurements, to ensure the accurate results of the average width of the fatigue stripes, five fatigue stripes were selected each time. One fatigue stripe was generated in one cycle, so $FGC_{rate}=L/d$, where L is measurement length of each of five fatigue stripes, and d is the number of stripes (i.e., 5). The FGC rates were respectively 1.76×10^{-4}, 2.16×10^{-4}, 2.52×10^{-4} and 3.54×10^{-4} mm/cycle under the corresponding pre-rolling conditions. In general, the smaller the distance between fatigue stripes, the lower the FCG rate.

Figure 12 displays the SEM images of the fracture surface morphologies at the final instantaneous rupture zone of the alloys under different pre-rolling conditions. It can be seen from the figure that almost all the fractures were intergranular fractures, which is consistent with the characteristics of the tensile fracture surfaces shown in Figure 8.

3.4 Dispersion of precipitates

As shown in Figures 13 and 14, the T_1 phase, which is the main strengthening phase in Al-Li alloys [22] was obvious in the 2195 alloy specimens under the four pre-rolling conditions, and with the increase of pre-rolling, the T_1 phase became denser and finer. Moreover, as can be seen from Figure 14, the amount of the S' phase in the alloy also significantly increased with the increase of pre-rolling from 0 to 9%. As dislocation slip occurs in the grains, the mutual reaction of dispersed precipitates and dislocations will cause the dislocations to be blocked and pinned, resulting in the reinforcement of the alloy [26, 27]. In addition, according to research conducted by ZHAO et al [28, 29], the amount of the T_1 phase has a great influence on the increase of the strength and hardness of the alloy by changing its texture.

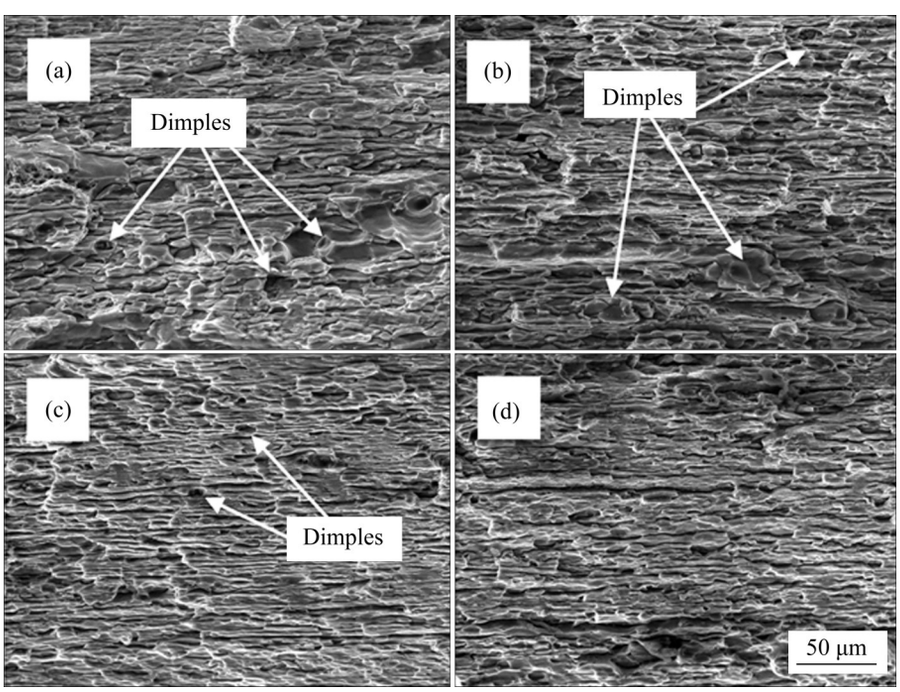

Figure 12 SEM images of fracture morphologies at final instantaneous rupture zone of 2195 Al-Li alloy specimens under different degrees of pre-rolling: (a) 0; (b) 3%;(c) 6%; (d) 9%

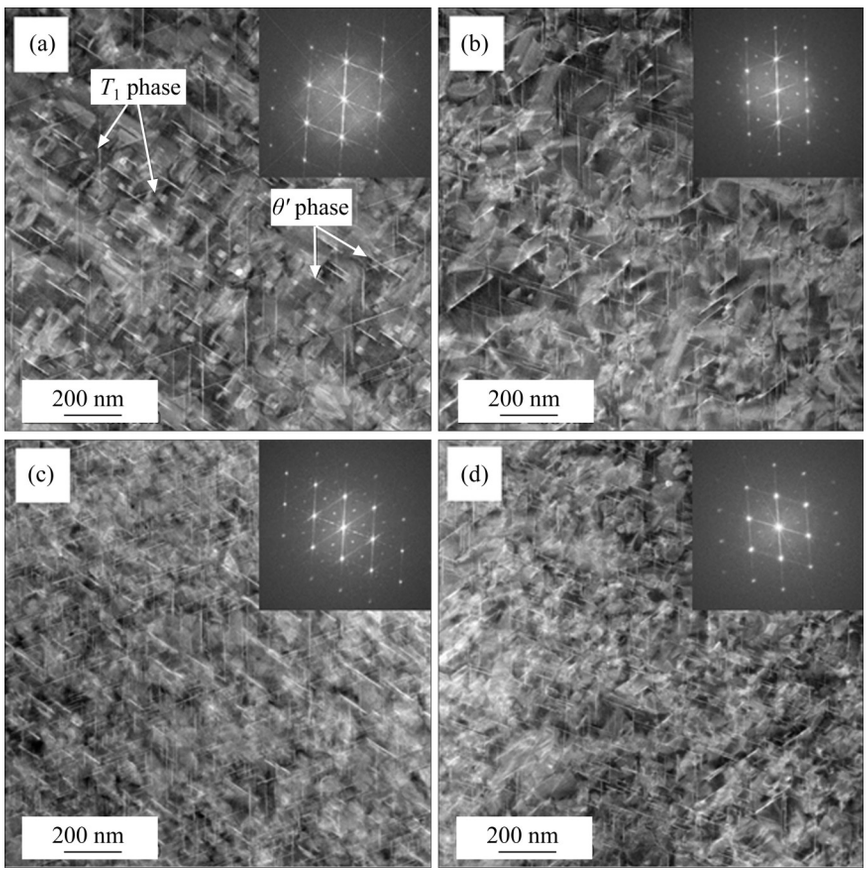

Figure 13 STEM bright-field images of T_1 and θ' phases in 2195 Al-Li alloy specimens under different degrees of pre-rolling, b=<110>$_\alpha$: (a) 0; (b) 3%; (c) 6%; (d) 9%

During the pre-rolling process, plastic deformation leads to a significant increase in the dislocation density. Dislocation tangles make the grain boundary difficult to move, and reduce the ductility of the alloy. By performing aging treatment after rolling, precipitates, such as S' precipitates, develop and result in pinning dislocation and increase dislocation glide resistance, and further lead to the poor ductility and fatigue resistance of the alloy [30].

Furthermore, the volume of the T_1 phase was also found to change greatly with the increase of the degree of pre-rolling. As shown in Figure 13, the mean length of the T_1 phase in the specimen without pre-rolling was 264.5 nm, while those in the specimens pre-rolled at 3%, 6% and 9% were respectively 139.2, 101.8 and 82.1 nm. According to LI et al [31−33] and WU et al [34], the size of the T_1 phase has a great influence on the intensity of textures of Al alloys; the decrease in the volume of the T_1 phase leads to a decrease in the intensity of the Goss texture and an increase in the intensity of the Brass texture. Because the twist angle of the grain boundary between the texture grain and the adjacent grain of the Brass texture is much smaller than that of the Goss texture, with the increase of the degree of pre-rolling, the average twist angle is reduced and leads to the weak deflection of the crack; moreover, cracks tend more easier to pass through the grain, thereby increasing the FCG rate.

4 Conclusions

In this study, the microstructures, mechanical properties, and fatigue resistances of 2195 Al-Li alloy specimens under different pre-rolling conditions were investigated, and the main conclusions are as follows.

1) The hardness of the alloy was found to increase with the increase of the degree of pre-rolling. When the pre-rolling deformation was 9%, the hardness of the specimen was HV 186.81, which was 13.9% higher than that of the specimen without pre-rolling. Furthermore, pre-rolling changed the

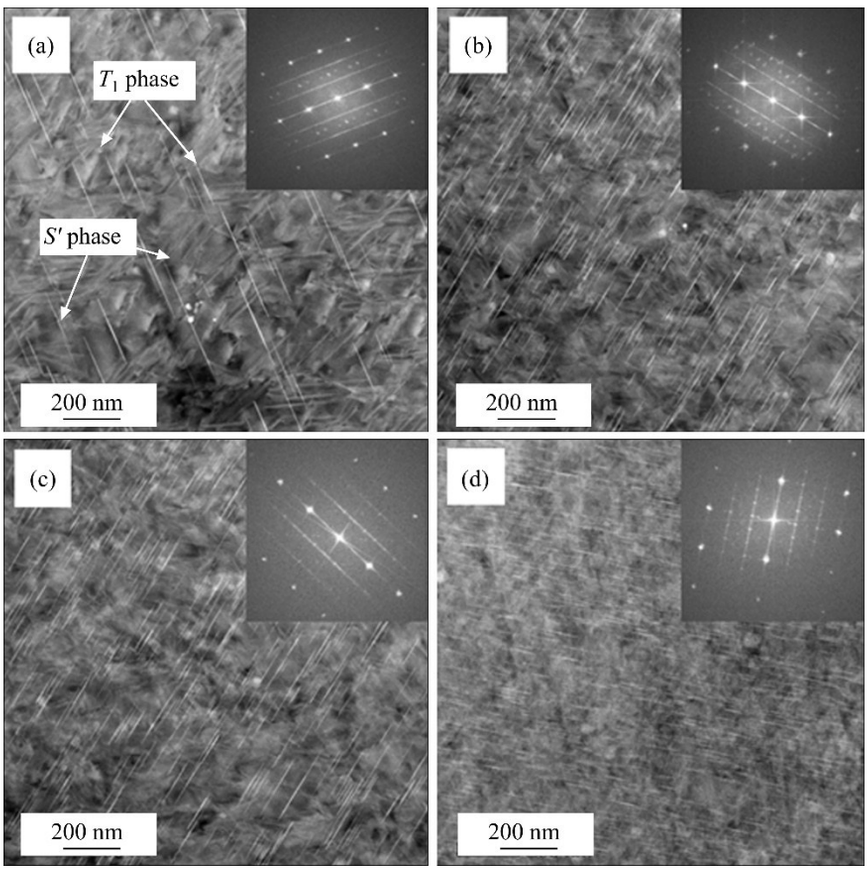

Figure 14 STEM bright-field images of T_1 and S' phases in 2195 Al-Li alloy specimens under different degrees of pre-rolling, b=<112>$_\alpha$: (a) 0; (b) 3%; (c) 6%; (d) 9%

other mechanical properties of the 2195 Al-Li alloy specimens; with the increase of pre-rolling, the tensile strength and yield strength of the specimens increased, but the elongation decreased. When the degree of pre-rolling deformation was 9%, the tensile strength and yield strength of the specimen were respectively 641 and 605 MPa, and the elongation was 9.3%.

2) The degree of pre-rolling obviously affected the FGC resistance of the specimens. At the 95% confidence level, pre-rolling deformation of 3%, 6%, and 9% led to decrease in the fatigue life of the alloy of 5.94%−23.29%, 5.2%−29.93% and 7.59%−35.9%, respectively.

3) The normalized stress intensity factor $\Delta K/E$ was introduced to correlate the Paris-type relation for the prediction of the crack growth rate of 2195 Al-Li alloy specimens under different pre-rolling conditions. It was found that the fatigue properties of the specimens after pre-rolling can be better characterized by E.

4) Pre-rolling was found to increase the distances between two fatigue stripes, leading to the smaller size of the T_1 phase and a smaller twist angle, which reduced the fatigue resistance of the specimens. However, with the increase of the degree of pre-rolling, the increases of the fine T_1 phase and S' precipitates led to increases in both the hardness and strength of the 2195 Al-Li specimens.

Contributor

The overarching research goals were formulated by LI Yi-bo, CHEN Meng-xi, and HUANG Ming-hui. CHEN Meng-xi, XIA Lin-yan, and WU Zhen-yu provided the measured mechanical performance data and analyzed the measured data. LI Yi-bo, CHEN Meng-xi, and XIA Lin-yan provided the results of fatigue crack growth experiments and performed calculations and analyses on the results. YANG Yi and QU Zi-jing assisted in the preparation of all test samples. The first draft was written by LI Yi-bo, CHEN Meng-xi, and XIA Lin-yan. All authors responded to the reviewers' comments and revised the final version.

Conflict of interest

CHEN Meng-xi, LI Yi-bo, XIA Lin-yan, HUANG Ming-hui, WU Zhen-yu, YANG Yi, QU Zi-jing declare that they have no conflict of interest.

References

[1] XIOMARA C, THOMAS B, RIOJA R J. New aluminum lithium alloys for aerospace applications [C]// Light Met Technol Conf. Quebec, Canada: Saint-Saveur, 2007: 41−46.

[2] RIOJA R J, LIU J. The evolution of Al-Li base products for aerospace and space applications [J]. Metallurgical and Materials Transactions A, 2012, 43(9): 3325 − 3337. DOI: 10.1007/s11661-012-1155-z.

[3] WARNER T. Recently-developed aluminium solutions for aerospace applications [J]. Materials Science Forum, 2006, 519−521: 1271−1278. DOI: 0.4028/www.scientific.net/msf.519-521.1271.

[4] MARSH G. Composites and metals − A marriage of convenience? [J]. Reinforced Plastics, 2014, 58(2): 38 − 42. DOI: 10.1016/s0034-3617(14)70108-0.

[5] YUAN Shun, LI Yi-bo, HUANG Ming-hui, et al. Determination of key parameters of Al‒Li alloy adhesively bonded joints using cohesive zone model [J]. Journal of Central South University, 2018, 25(9): 2049 − 2057. DOI: 10.1007/s11771-018-3894-5.

[6] RIOJA R J. Fabrication methods to manufacture isotropic Al-Li alloys and products for space and aerospace applications [J]. Materials Science and Engineering A, 1998, 257(1): 100−107. DOI: 10.1016/S0921-5093(98)00827-2.

[7] ZHOU C, ZHAN L H, SHEN R L, et al. Creep behavior and mechanical properties of Al-Li-S4 alloy at different aging temperatures [J]. Journal of Central South University, 2020, 27(4): 1168−1175. DOI: 10.1007/s11771-020-4357-3.

[8] WEN Tao, CHEN Yong-lai, DU Yue, et al. Effect of spinning-deformation on microstructure and mechanical properties in 2195 Al-Li alloy [J]. Manned Spaceflight, 2020, 26(6): 717−722. DOI: 10.3969/j.issn.1674-5825.2020.06.007.

[9] DUAN Lian, ZHAN Li-hua, XU Yong-qian, et al. Effect of pre deformation on creep aging behavior and microstructure evolution of Al-Li alloy [J]. Journal of Plastic Engineering, 2020, 27(8): 106−115.

[10] WANG Lin, BHATTA L, XIONG Han-qing, et al. Mechanical properties and microstructure evolution of an Al-Cu-Li alloy subjected to rolling and aging [J]. Journal of Central South University, 2021, 28: 3800−3817. DOI: https://doi.org/10.1007/s11771-021-4764-0.

[11] STARKE E A, STALEY J T. Application of modern aluminum alloys to aircraft [J]. Progress in Aerospace Sciences, 1996, 32(2, 3): 131−172.

[12] SCHIJVE J. The effect of pre-strain on fatigue crack growth and crack closure [J]. Engineering Fracture Mechanics, 1975, 8(4):575−581.

[13] WANG Zhi-xiu, LI Hai, WEI Xiu-yu, et al. Effects of prior strain on static tensile properties and fatigue lives of 2E12 aluminum alloy [J]. Rare Metal Materials and Engineering, 2010, 39(S1): 138−141. (in Chinese)

[14] LIU Fei, LIU Zhi-yi, LIU Meng, et al. Analysis of empirical relation between microstructure, texture evolution and fatigue properties of an Al-Cu-Li alloy during different pre-deformation processes [J]. Materials Science and Engineering A, 2018, 726: 309 − 319. DOI: 10.1016/j.msea.2018.04.047.

[15] SHEN Ke-ren, TIMKO M, LI Yong-jun, et al. The effect of temper, grain orientation, and composition on the fatigue properties of forged aluminum-lithium 2195 alloy [J]. Journal of Materials Engineering and Performance, 2019, 28(9): 5625−5638. DOI: 10.1007/s11665-019-04300-y.

[16] GABLE B M, ZHU A W, CSONTOS A A, et al. The role of plastic deformation on the competitive microstructural evolution and mechanical properties of a novel Al-Li-Cu-X alloy [J]. Journal of Light Metals, 2001, 1(1): 1 − 14. DOI: 10.1016/S1471-5317(00)00002-X.

[17] CASSADA W A, SHIFLET G J, STARKE E A. The effect of plastic deformation on Al_2CuLi (T_1) precipitation [J]. Metallurgical Transactions A, 1991, 22(2): 299 − 306. DOI: 10.1007/BF02656799.

[18] ZHANG Jin, LI Zhi-de, XU Fu-shun, et al. Regulating effect of pre-stretching degree on the creep aging process of Al-Cu-Li alloy [J]. Materials Science and Engineering A, 2019, 763: 138157. DOI: 10.1016/j.msea.2019.138157.

[19] LI Jin-feng, YE Zhi-hao, LIU Dan-yang, et al. Influence of pre-deformation on aging precipitation behavior of three Al-Cu-Li alloys [J]. Acta Metallurgica Sinica (English Letters), 2017, 30(2): 133 − 145. DOI: 10.1007/s40195-016-0519-6.

[20] PEARSON S. Fatigue crack propagation in metals [J]. Nature, 1966, 211(5053): 1077 ‒ 1078.

[21] LAL D N. On the combined influences of Young's modulus and stress ratio on the LEFM fatigue crack growth process: A new mechanistic approach [J]. Engineering Fracture Mechanics, 1996, 54(6): 761 − 790. DOI: 10.1016/0013-7944(95)00240-5.

[22] MATCHA N B, SASIKALA G. Effect of temperature on the fatigue crack growth behaviour of SS316L(N) [J]. International Journal of Fatigue, 2020, 40: 105815.

[23] MURAYAMA M, HONO K, SAGA AND M, et al. Atom probe studies on the early stages of precipitation in Al-Mg-Si alloys [J]. Materials Science and Engineering A, 1998, 250(1): 127.

[24] RITCHIE R O. Near-threshold fatigue-crack propagation in steels [J]. International Metals Reviews, 1979, 24(1): 205 − 230. DOI: 10.1179/imtr.1979.24.1.205.

[25] RODGERS B I, PRANGNELL P B. Quantification of the influence of increased pre-stretching on microstructure-strength relationships in the Al-Cu-Li alloy AA2195 [J]. Acta Materialia, 2016, 108: 55 − 67. DOI: 10.1016/j.actamat.2016.02.017.

[26] AN Li-hui, CAI Yang, LIU Wei, et al. Effect of pre-deformation on microstructure and mechanical properties of 2219 aluminum alloy sheet by thermomechanical treatment [J]. Transactions of Nonferrous Metals Society of China, 2012, 22: s370−s375. DOI: 10.1016/S1003-6326(12)61733-6.

[27] DORIN T, de GEUSER F, LEFEBVRE W, et al. Strengthening mechanisms of T_1 precipitates and their

influence on the plasticity of an Al-Cu-Li alloy [J]. Materials Science and Engineering A, 2014, 605: 119 − 126. DOI: 10.1016/j.msea.2014.03.024.

[28] ZHAO Qi, LIU Zhi-yi, LI Sha-sha, et al. Evolution of the Brass texture in an Al-Cu-Mg alloy during hot rolling [J]. Journal of Alloys and Compounds, 2017, 691: 786 − 799. DOI: 10.1016/j.jallcom.2016.08.322.

[29] ZHAO Qi, LIU Zhi-yi, HUANG Tian-tian, et al. Enhanced fracture toughness in an annealed Al-Cu-Mg alloy by increasing Goss/Brass texture ratio [J]. Materials Characterization, 2016, 119: 47−54. DOI: 10.1016/j.matchar.2016.07.015.

[30] WANG Z C, PRANGNELL P B. Microstructure refinement and mechanical properties of severely deformed Al-Mg-Li alloys [J]. Materials Science and Engineering A, 2002, 328(1, 2): 87−97. DOI: 10.1016/S0921-5093(01)01681-1.

[31] LI Fu-dong, LIU Zhi-yi, WU Wen-ting, et al. Enhanced fatigue crack propagation resistance of Al-Cu-Mg alloy by intensifying Goss texture and refining Goss grains [J]. Materials Science and Engineering A, 2017, 679: 204−214. DOI: 10.1016/j.msea.2016.10.003.

[32] LI Fu-dong, LIU Zhi-yi, WU Wen-ting, et al. Slip band formation in plastic deformation zone at crack tip in fatigue stage II of 2xxx aluminum alloys [J]. International Journal of Fatigue, 2016, 91: 68 − 78. DOI: 10.1016/j. ijfatigue. 2016. 05.014.

[33] LI Fu-dong, LIU Zhi-yi, WU Wen-ting, et al. On the role of texture in governing fatigue crack propagation behavior of 2524 aluminum alloy [J]. Materials Science and Engineering A, 2016, 669: 367−378. DOI: 10.1016/j.msea.2016.05.091.

[34] WU Wen-ting, LIU Zhi-yi, HU Yang-cheng, et al. Goss texture intensity effect on fatigue crack propagation resistance in an Al-Cu-Mg alloy [J]. Journal of Alloys and Compounds, 2018, 730: 318 − 326. DOI: 10.1016/j. jallcom. 2017.09.320.

(Edited by HE Yun-bin)

中文导读

预变形对2195铝锂合金力学性能及疲劳裂纹扩展速率的影响

摘要：时效前的预变形处理可增加2195铝锂合金的强度和硬度，但这会加快合金的疲劳裂纹扩展(FCG)速率，从而缩短合金的疲劳寿命。确定合适的预变形-时效工艺制度，在提高2195铝锂合金的强度和硬度的同时尽量降低其对疲劳裂纹扩展速率的影响，是进一步提高铝锂合金服役性能的关键。为此，研究了预变形程度(0、3%、6%和9%)对2195铝锂合金试样的硬度、强度、裂纹扩展速率以及疲劳断裂形貌与析出相等影响规律，揭示预变形对2195铝锂合金力学性能和FCG速率影响的作用机制。结果表明：随着预变形量的增加，T_1相密度增加、S'相分布细化，导致合金显微硬度、抗拉强度和屈服强度增加，同时FCG速率加快、合金疲劳寿命缩短。同时，还提供了不同预变形程度下2195铝锂合金FCG速率的计算模型，将弹性模量(E)作为归一化应力强度因子，实现预变形后2195铝锂合金的FCG速率与常数C和K相关联，较好地预测了不同预变形状态下2195铝锂合金的裂纹扩展速率。

关键词：2195铝锂合金；预变形；过时效；疲劳裂纹扩展；力学性能